



Experimental Study on Elasto-Plastic Behavior of R/C Exterior Beam-Column Joints with Parameters of Varying Axial Forces and Lateral Reinforcements

Y. Suzuki⁽¹⁾, M. Maeda⁽²⁾, T. Ohta⁽³⁾, J. Sakuta⁽⁴⁾, T. Kiyohara⁽⁵⁾, K. Fujiwara⁽⁶⁾

⁽¹⁾ Assistant Professor, Graduate School of Engineering, Osaka City University, ysuzuki@arch.eng.osaka-cu.ac.jp

⁽²⁾ Professor, Graduate School of Engineering, Tohoku University, maeda@rcl.archi.tohoku.ac.jp

⁽³⁾ Maeda Corporation, tetsu.ohta2@gmail.com

⁽⁴⁾ Horie Engineering and Architectural Research Institute Co.,Ltd, sakuta@horieken.co.jp

⁽⁵⁾ Horie Engineering and Architectural Research Institute Co.,Ltd, kiyohara@horieken.co.jp

⁽⁶⁾ Suzuki Architectural Design Office, gr2k-fjwr@asahi-net.or.jp

Abstract

In the Japanese seismic design criteria for beam-column joint of reinforced concrete frame structures with beam yielding, it is restricted that the shear force at the joint panel does not exceed the shear strength of joint on basis of past experimental data. However, in recent research (Dr. Shiohara's studies), it was shown that the maximum strength of frame structures with the beam yielding total collapse mechanism does not achieve the expected design strength (beam bending strength) due to joint panels eventually collapse; this may occur even when frame structures satisfy the current seismic design standards if column-to-beam bending strength margin of the frame structure is less than 2.0. On the other hand, it was found, through an experimental study that it is possible to reduce the damage to the joint panels and achieve the design strength of the structural frame when increasing confinement of joint panel by lateral reinforcements and applying low level constant compressive axial loading to the columns, for the exterior beam-column joint in a frame structure with column-to-beam bending strength margin of approximately 1.5.

The objective of this study is to clarify seismic performance of exterior beam-column joint structures with column-to-beam bending strength margin of less than 1.5 when the structure is subjected to high level varying axial forces (an axial force ratio of 0.6 in tension to 0.5 in compression). In addition, the purpose of this study is to establish stiffening effects of lateral reinforcements in the joint panel.

Six identical 1/2-scale models of exterior beam-column joint specimens with two levels of column-to-beam bending strength ratios (approximately 1.2 or 1.5) were prepared. Experimental parameters of six test specimens were column-to-beam bending strength ratio, axial stress level and lateral reinforcements of joint panel. In terms of loading method that assumed seismic forces, the test specimen was subjected to static horizontal cyclic loading at the top of the column. Simultaneously, a varying axial load proportional to the beam shear forces was applied.

From the experimental results, it is revealed how varying axial forces affect structural performances in terms of damage on joint panel, strength, deformation capacities, and failure mechanisms of structures; it was also possible to verify whether using lateral reinforcements improved the performance of structures.

Keywords: Beam-column joints, Column-to-beam bending strength ratio, Varying axial forces, Lateral Reinforcements

1. Introduction

Destruction of a beam-column joint in a reinforced concrete construction building is a critical failure mode that may lead to collapse of the building. In the current seismic design criteria for the beam-column joint of reinforced concrete frame structures with a beam yielding total collapse mechanism, it is restricted that the shear force at the joint panel does not exceed the shear strength of joint panel on basis of past experimental data ^[1]. In the recent research of Dr. Shiohara, et al. (2012 ^[2], 2013 ^[3]), it was shown that the maximum strength of the frame structures with a total collapse mechanism (beam yielding) does not achieve the design expected strength, as shown in Fig. 1 (past experimental data are referenced in Table 4), and joint panels may eventually collapse if



column-to-beam bending strength ratio of the frame structure is less than 2.0. This may occur even when the frame structures satisfy current seismic design standards^[1].

On the other hand, the authors explained through an experimental study that it is possible to reduce the damage to joint panels and achieve the design strength of structural frame with a column-to-beam bending strength ratio of approximately 1.5^[4]. This can be accomplished by increasing the amounts and strengthening of the lateral reinforcements in the joint panel or applying low-level compressive axial loading to the columns for the exterior beam-column joint structure. In addition, the progress of the deformation and damage in a beam-column joint panel was observed for a low-level tensile axial force applied to a specimen^[4]. When a high-rise building is subjected to a severe seismic force, high-level varying axial force is repeatedly applied to the exterior beam-column joint structure of lower story of the building. However, there are a number of unclarified points regarding the structural performance of the beam-column joint structure when a high-level varying axial force is applied.

In this research, the seismic performance of an exterior beam-column joint structure with a column-to-beam bending strength ratio of less than 1.5 is clarified when the structure is subjected to high-level varying axial forces (an axial force ratio of 0.6 in tension to 0.5 in compression). In addition, the stiffening effects of the lateral reinforcements in the joint panel are investigated.

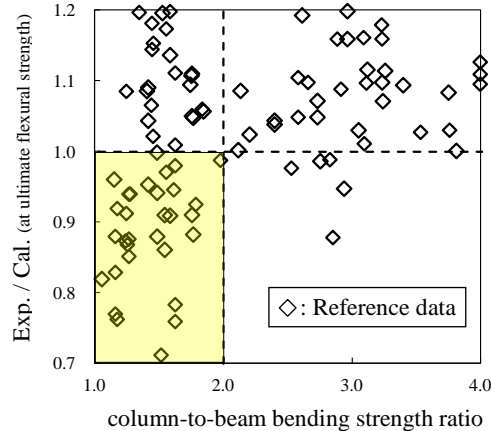


Fig. 1 – Exp./Cal. Versus the column-to-beam bending strength ratio

2. Experimental Program

2.1 Details of the R/C Beam-Column Joint Specimens and Test Parameters

Table 1 summarizes specifications and reinforcement details of beam-column joint specimens and test parameters. Fig. 2 illustrates the geometry, size, and reinforcement arrangement of the specimen (T15-50TC5). Each calculated value is also listed in the Table 1. Six identical 1/2-scale models of the exterior beam-column joint specimens were prepared with a column cross section of 250 mm × 250 mm and a beam cross section of 225 mm × 275 mm. All of the exterior beam-column joint specimens were sub-structures derived from a lower story of high-rise R/C frame buildings designed with beam yielding collapse mechanism (with a joint shear margin of more than 1.0) according to the design guidelines of the AIJ standard^[1]. Inflection point of beams and columns were assumed at mid-span and mid-height, respectively and pin joints were attached at the ends of beams and columns as locations of pins agree with the inflection points.

The test parameters were the (1) column-to-beam bending strength ratio, (2) axial force, and (3) joint reinforcement ratio, as shown in Fig. 3. The column-to-beam bending strength ratio was arranged about 1.5 or 1.2 in tension side (when the specimen was subjected to the maximum tensile axial force with a ratio of 0.6), so that the joint yielding proceeds in advance of beam flexural yielding according to Dr. Shiohara's theory. The varying axial force is selected ranging from a tensile axial force ratio of 0.6 to compressive axial force ratio of 0.3 (approximately the equilibrated axial force) or 0.5, in order to observe damage progress in the panel zone and

vertical load carrying capacity after damage in joint under high-level tensile and compressive axial force reversal. That is, the application of a high-level varying axial force is confirmed to affect the structural performance of the beam-column joint specimens. Here, compressive and tensile axial force ratio was defined as $\sigma_B \times A / N$ (σ_B : concrete compressive strength, A : cross section of column, N : axial force) and $c\sigma_y \times \Sigma a / N$ ($c\sigma_y$: yield strength of column main reinforcement, Σa : total cross section of column main reinforcement), respectively. The joint reinforcement ratio (T_h/T_{by}) defined by Fig.3 was arranged about 0.2 or 0.5 in order to confirm the effect of lateral confinement on improvement of structural performance of joint panel.

Table 1 – Specifications and reinforcement details of the test specimens

| Type of Specimen | T15-50TC5 | T15-20TC5 | T15-20TC3 | T12-50TC5 | T12-20TC5 | T12-20TC3 | |
|---|---|-------------------|-------------------|-------------------|-------------------|-----------|-------|
| $H \times L$ | 1,350 × 1,850 | | | | | | |
| Cross section (mm) | 250 × 250 | | | | | | |
| Main reinforcement | 12-D16 (SD490) | | | 12-D16 (SD345) | | | |
| $c p_t$ (%) | 1.91 | | | | | | |
| Hoop | 2-D6 (SD295) | | | | | | |
| $c p_w$ (%) | 0.51 | | | | | | |
| Story shear force at flexural ultimate (kN) | top (+ ⁻¹) | 297.0 | 297.4 | 312.8 | 287.5 | 284.8 | 283.0 |
| | | 111.8 | | 107.8 | 93.6 | 86.5 | 93.1 |
| | bottom (+) | 305.2 | 305.5 | 311.1 | 284.6 | 281.8 | 288.2 |
| | | 93.8 | | 89.5 | 75.6 | 68.5 | |
| Beam | Cross section (mm) | 225 × 275 | | | | | |
| | Main reinforcement (Mechanical anchor) | 5-D13 (SD490) | | | | | |
| | $b p_t$ (%) | 1.14 | | | | | |
| | Stirrup | 2-D6 (SD295) | | | | | |
| | $b p_w$ (%) | 0.84 | | | | | |
| | Story shear force at flexural ultimate (kN) | 65.7 | | 66.9 | 65.7 | 66.9 | 65.6 |
| Joint panel | Hoop | 4-D6 4set (SD345) | 2-D6 3set (SD295) | 4-D6 4set (SD345) | 2-D6 3set (SD295) | | |
| | $j p_w$ (%) | 0.93 | 0.35 | 0.93 | 0.35 | | |
| | Shear strength (kN) ¹ | 393.4 | 393.8 | 376.3 | 393.4 | 383.2 | 376.3 |
| beam-column bending strength ratio at | (+) loading | 4.51 | | 4.49 | 4.29 | 4.16 | 4.29 |
| | (-) loading | 1.54 | | | 1.27 | | |
| Joint reinforcement ratio | 0.5 | 0.2 | | 0.5 | 0.2 | | |
| Axial force ratio at | (+) loading | 0.47 | | 0.28 | 0.47 | 0.49 | 0.28 |
| | (-) loading | -0.63 | | | -0.61 | | |
| Joint shear margin | 1.31 | | 1.29 | 1.31 | 1.29 | 1.26 | |
| Anchor strength margin | 1.65 | | 1.64 | 1.38 | 1.37 | 1.38 | |

*1: (+) and (-) mean compressive and tensile axial loading in columns, respectively.

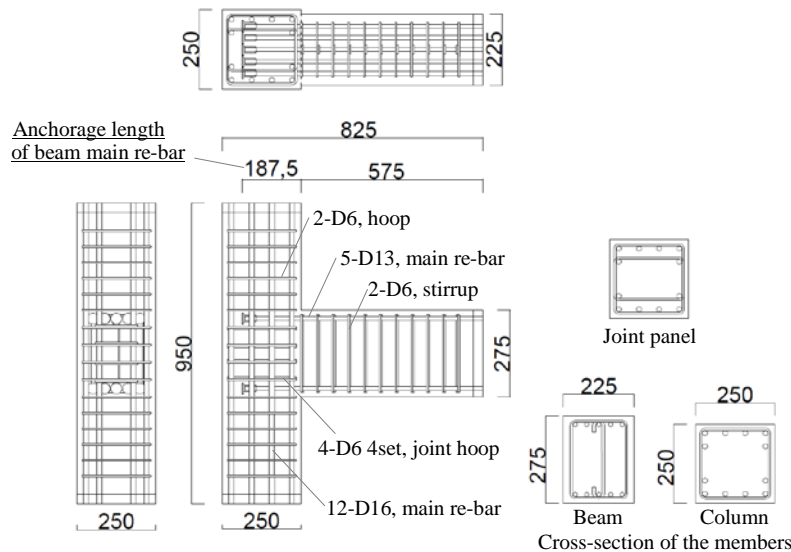
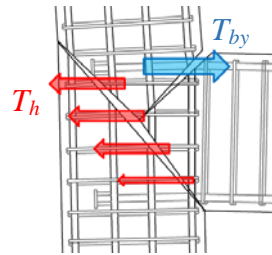


Fig. 2 – Details of the exterior beam-column joint specimen (T15-50TC5)

2.2 Materials

Table 2 and Table 3 show the properties of concrete and mechanical properties of steel bars, respectively. Concrete with a nominal compressive strength of $F_c = 50$ MPa was used for all specimens. The compressive strengths obtained by compressive tests of concrete cylinders with diameters of 100 mm ranged from 60.9 to 65.0 MPa. The yield strengths obtained by tensile tests of reinforcing bars are listed in Table 3.



$$\text{Joint reinforcement ratio} = T_h / T_{by}$$

T_h : yield strength of lateral reinforcement in joint panel

$$T_h = \sum a_w \times \sigma_{wy}$$

T_{by} : yield strength of beam main reinforcement

$$T_{by} = \sum a_t \times \sigma_{by}$$

Fig. 3 – Conceptual view of the joint reinforcement ratio

Table 2 – Properties of concrete

| Type of concrete (specimen) | Age (d) | Compressive strength (MPa) | Longitudinal strain (μ) | Young's modulus ($\times 10^4$ MPa) | Split tensile strength (MPa) |
|-----------------------------|---------|----------------------------|-------------------------------|--------------------------------------|------------------------------|
| T15-50TC5 | 84 | 64.9 | 2573 | 3.35 | 3.50 |
| T15-20TC5 | 81 | 65.0 | 2484 | 3.35 | 4.20 |
| T15-20TC3 | 57 | 65.4 | 2610 | 3.24 | 3.30 |
| T12-50TC5 | 75 | 64.9 | 2463 | 3.32 | 3.51 |
| T12-20TC5 | 50 | 64.9 | 2631 | 3.28 | 3.20 |
| T12-20TC3 | 47 | 60.9 | 2341 | 3.27 | 3.11 |

Table 3 – Mechanical properties of steel bars

(a) T15-50TC5, T15-20TC5, T12-50TC5, T12-20TC3

| Type of steel | | Yield strength (MPa) | Yield strain (μ) | Young's modulus ($\times 10^4$ MPa) | Tensile strength (MPa) |
|-----------------------|-----|----------------------|------------------------|--------------------------------------|------------------------|
| Hoop and Stirrup | D6 | SD295 | 409.4 | 1981 | 548.7 |
| | | SD345 | 392.7 | 2176 | 582.6 |
| Main re-bar of beam | D13 | SD490 | 529.3 | 2961 | 709.9 |
| Main re-bar of column | D16 | SD345 | 410.5 | 2175 | 589.3 |
| | | SD490 | 544.0 | 2908 | 732.6 |

(b) T15-20TC3, T12-20TC5

| Type of steel | | Yield strength (MPa) | Yield strain (μ) | Young's modulus ($\times 10^4$ MPa) | Tensile strength (MPa) |
|-----------------------|-----|----------------------|------------------------|--------------------------------------|------------------------|
| Hoop and Stirrup | D6 | SD295 | 433.8 | 2329 | 572.7 |
| Main re-bar of beam | D13 | SD490 | 536.6 | 2840 | 713.2 |
| Main re-bar of column | D16 | SD345 | 395.3 | 2050 | 562.4 |
| | | SD490 | 554.3 | 2876 | 737.6 |

2.3 Loading and Measuring Method

Fig. 4 and Fig. 5 show the loading setup and loading history respectively. The ends of columns and beam of a specimen were supported with a pin and pin roller, respectively, as shown in Fig. 4. For the loading method, the test specimen was subjected to horizontal static cyclic loading at the top of the column. Beam end was free in horizontal direction and fixed in vertical direction by vertical jack with two pins at both ends. Simultaneously, varying axial load proportional to the beam shear forces was applied to the specimen according to the relationship between axial force and beam shear force as shown in Fig. 6.

Story drift was measured as a horizontal relative displacement between top and bottom pins by displacement transducers fixed to aluminum-holder pin roller supported the column capital and base. The shear deformation of the joint panel was measured using displacement transducers in diagonal directions in the panel zone. The lateral and axial loads on column and the vertical reaction load at the end of beam were recorded by using load cells. The strain was measured at the respective load increments by strain gauges pasted to the main reinforcements of the column and beam, the hoops of the column, and the joint panel.

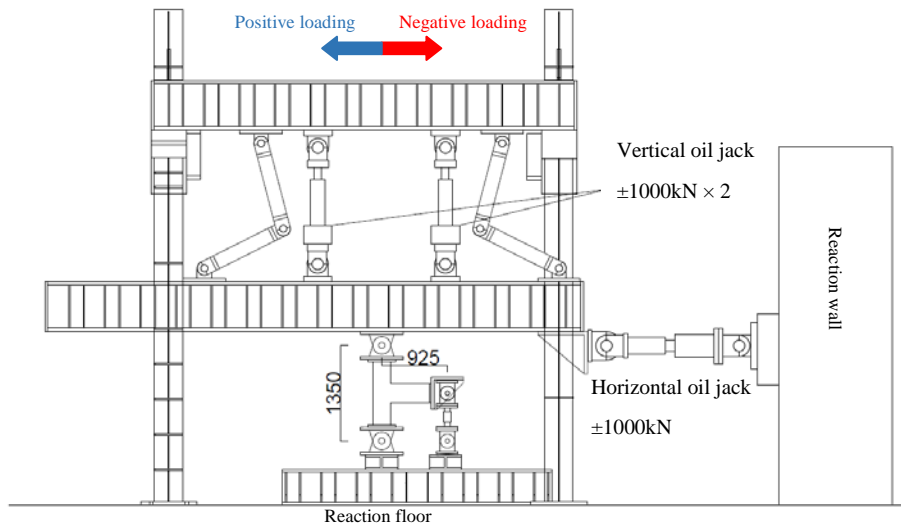


Fig. 4 – View of the loading setup

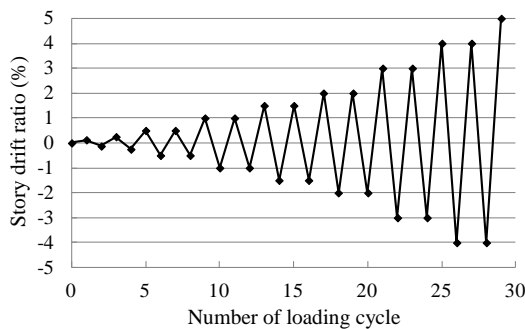


Fig. 5 – Loading history

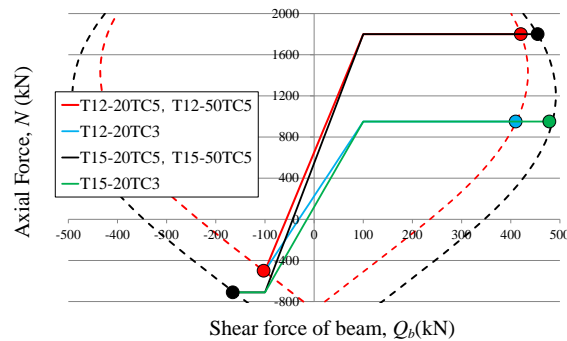


Fig. 6 – Loading method for varying axial force

3. Experimental Results and Discussion

3.1 Relationship between Story Shear Force - Story Drift Angle

Fig. 7 shows the story shear force and story drift angle relations. In all the specimens, yielding of longitudinal reinforcement in beam was observed at a story drift angle of about 1.0% under positive loading (compressive axial load in columns). On the other hand, yielding of hoops in joint panel was observed in advance of beam

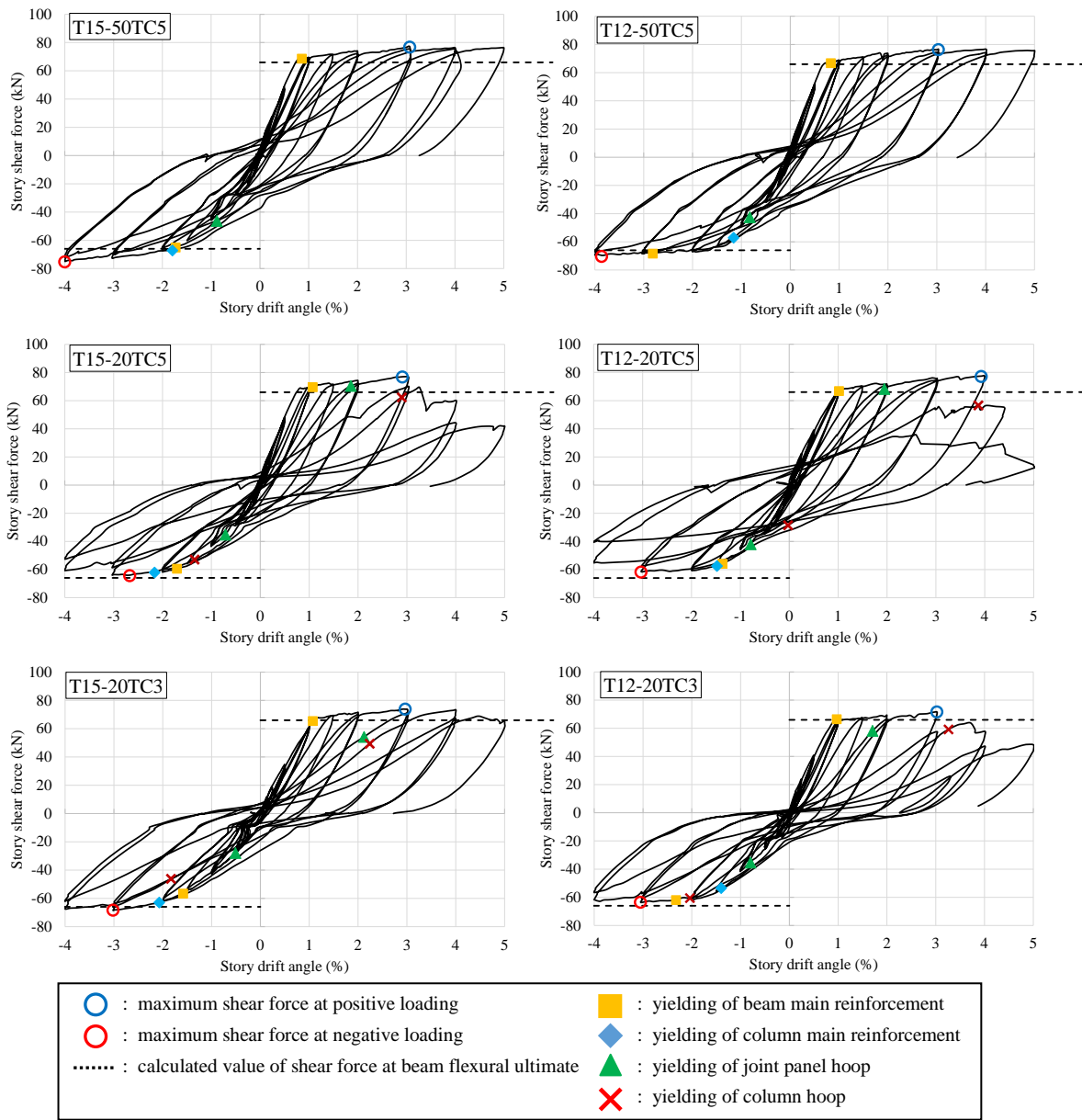


Fig. 7 – Story shear force and story drift angle curves of specimens

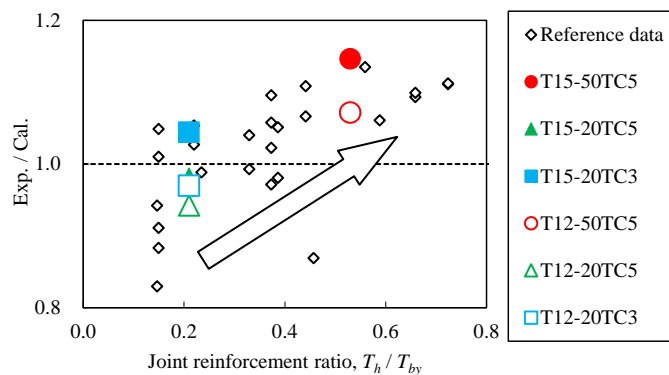


Fig. 8 – Exp. / cal. vs. joint reinforcement ratio of specimens at negative loading



flexural yielding under tensile axial load in column with which column-to-beam bending strength margin is lower than 1.5. Furthermore, the maximum force experienced by the T15-20TC5, T12-20TC5 and T12-20TC3 specimens under negative loading did not reach the story shear force expected by ultimate flexural strength of beam yielding. The behaviors in the positive and negative loading directions were significantly different because high-level varying axial force affect failure mode of specimen. By comparing the joint reinforcement ratios (T_h/T_{by}) of 0.2 and 0.5, effect of confinement of joint panel was obvious; specimens with $T_h/T_{by} \approx 0.2$, except T15-20TC3, exhibited a significant decrease in story shear and axial load carrying capacity in positive loading direction after story drift of 3%. However, the specimens with $T_h/T_{by} \approx 0.5$ maintained both story shear and axial load up to larger story drift of 5%. In addition, even if the column-to-beam bending strength ratio is less than 2.0 (under negative loading of the specimens), it was found that an increase in the joint reinforcement ratio lead to a higher maximum shear load, as shown in Fig. 8 (past experimental data are referenced in Table 4). Here, Exp. is the experimental value of the maximum story shear force, and Cal. is the calculated value of the shear force at the ultimate flexural strength of the beam.

3.2 Development of Deformation and Crack Width in a Joint Panel and the Ultimate Failure Mode of the Specimen

This section reports the results of only three specimens with a column-to-beam bending strength ratio of 1.2 (T12-50TC5, T12-20TC5, and T12-20TC3) because similar tendency was observed in the specimens with the ratio of 1.5t.

Fig. 9 shows the shear stress and shear strain of the joint panel of beam-column specimens. All of the specimens exhibited a degrading of shear stiffness right after diagonal cracking occurred at the center of the joint panel (and the panel hoops yielded) under tensile axial load. In the early stage of loading, shear deformation increased only in the negative direction because of joint yielding. In the positive direction, major deformation component was flexural deformation in beam, although large shear deformation occurred in specimen T12-20TC5 at ultimate stage of story drift of 1/20 at which joint was crushed by high axial compressive load.

Fig. 10 shows the observed residual crack width in the beam and joint panel after $R = \pm 1/800, \pm 1/400, \pm 1/200, \pm 1/100, \pm 1/67, \text{ and } \pm 1/50$ cycles. The crack width was the maximum width measured after each positive and negative loading cycle. Under the negative loading (specimens were subjected to a tensile axial force), the crack width of the joint panel expanded at $R = -1/100$, exceeding the drift angle of approximately joint panel hoop yielding as shown in Fig. 7. In the positive loading, the crack width of the beam rapidly expanded after story drift $R = 1/200$ or $1/100$ at which beam flexural yielding occurred. An expansion of the diagonal crack width in the panel zone was hardly observed for all the specimens until $R = 1/50$ as a result of confinement joint panel by the compressive axial force.

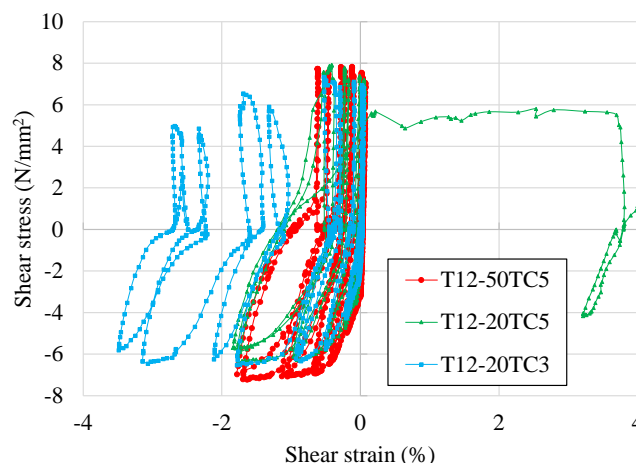


Fig. 9 – Shear stress and shear strain of joint panel

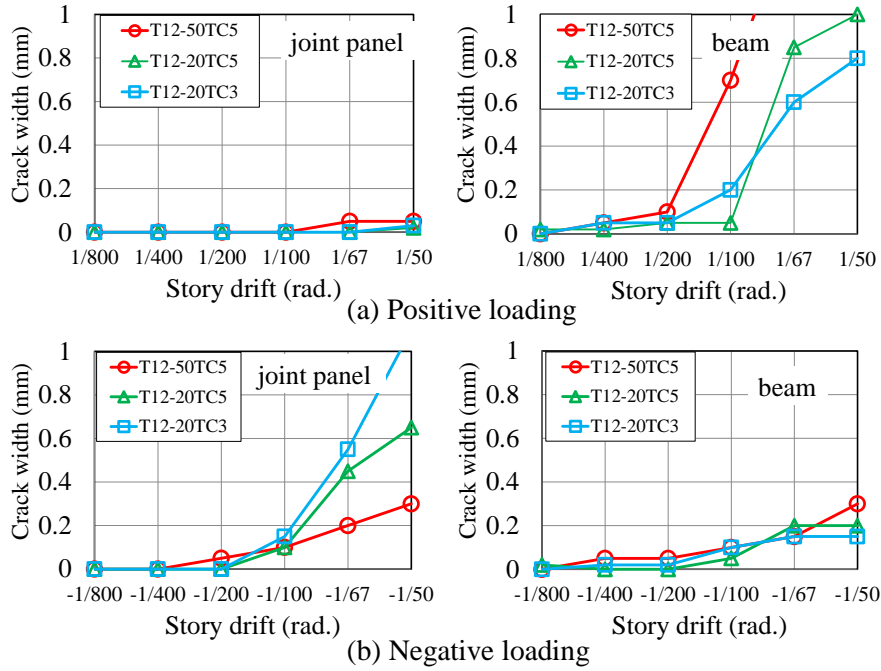


Fig. 10 – Observed residual crack width

Decrement of compressive axial force at the positive loading

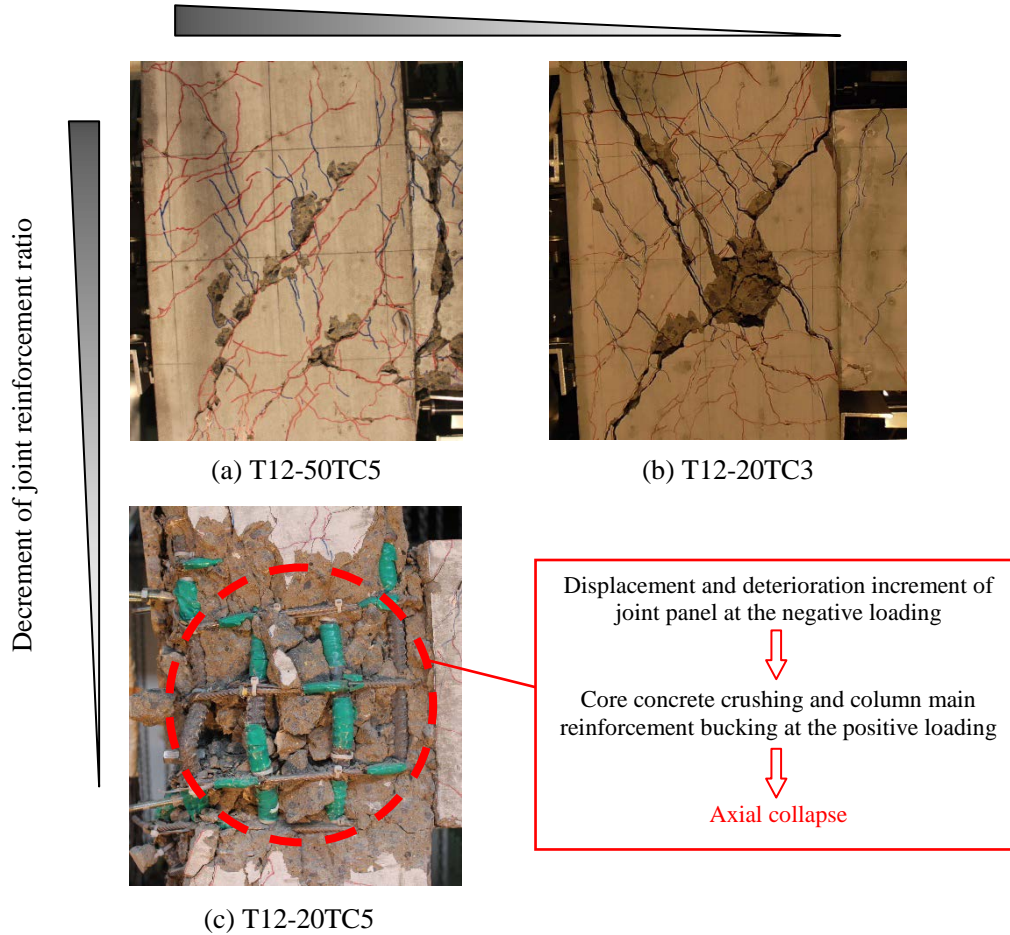


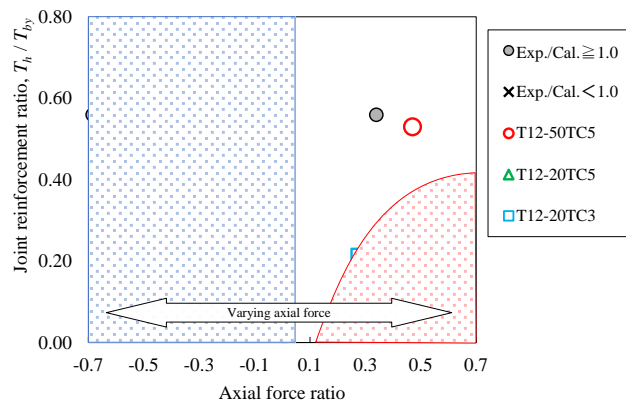
Fig. 11 – Ultimate failure modes



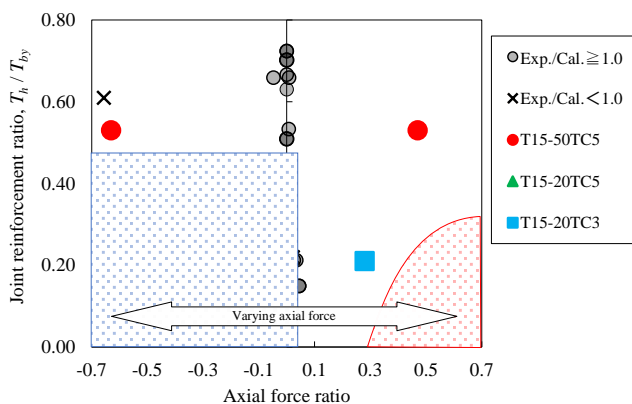
Fig. 11 shows the photographs at the ultimate failure mode ($R = 1/20$ rad.) of the joint panel zone. From the ultimate failure mode of the T12-20TC3 specimen, a large number of shear cracks with large widths was observed in the joint panel. In addition, the crushing of concrete was observed in the compressive strut zone. In comparison to the T12-20TC3 specimen, the diagonal cracks in the joint panel of the T12-50TC5 specimen were reduced as a result of the controlling effect of the joint panel lateral reinforcements. Finally, the T12-50TC5 specimen reached the safety failure mode with a ductility capacity. On the other hand, the T12-20TC5 specimen reached the most severe critical failure. Diagonal cracks with significant widths were observed in the panel zone, and all of the lateral reinforcements in the joint panel yielded during negative loading. Then, the specimen exhibited axial collapse under positive loading with the corresponding crushing of the core concrete and buckling of the column main reinforcement. It was demonstrated that when the R/C frame structure with a column-to-beam bending strength ratio of 1.5 or less and a joint reinforcement ratio of 0.2 or less was subjected to a high-level varying axial force, the structure might reach axial collapse.

4. Influence of Joint Reinforcement Ratio and Varying Axial Force for Beam-Column Joint Structure

As discussed previously, the varying axial force and joint reinforcement ratio are important factors that affect the structural performance of a beam-column joint structure with a smaller column-to-beam bending strength ratio less than 1.5. This section discusses the relationships between three parameters that affect seismic performance of beam-column joint structures.



(a) $1.0 < \text{column-to-beam bending strength ratio} \leq 1.3$



(b) $1.3 < \text{column-to-beam bending strength ratio} \leq 1.8$

Table 4 – List of reference data

| author | source | year | pp. |
|--------------------|--|------|-----------|
| Ogura, et al. | Summaries of technical papers of Annual Meeting, AIJ | 1976 | 1469/1470 |
| Kishida, et al. | Summaries of technical papers of Annual Meeting, AIJ | 1978 | 1683/1684 |
| Ogura, et al. | Summaries of technical papers of Annual Meeting, AIJ | 1987 | 641/642 |
| Ogura, et al. | Summaries of technical papers of Annual Meeting, AIJ | 1988 | 459/460 |
| Ybuchi, et al. | Summaries of technical papers of Annual Meeting, AIJ | 1993 | 257/258 |
| Miyazaki, et al. | Proceeding of the JapanConcrete Institute | 1994 | 717/722 |
| Murai, et al. | Summaries of technical papers of Annual Meeting, AIJ | 1994 | 683/686 |
| Kubota, et al. | Proceeding of the JapanConcrete Institute | 1995 | 1189/1194 |
| Kawasaki, et al. | Summaries of technical papers of Annual Meeting, AIJ | 1995 | 67/68 |
| Sakata, et al. | Summaries of technical papers of Annual Meeting, AIJ | 1995 | 45/46 |
| Fuji, et al. | Proceeding of the JapanConcrete Institute | 1996 | 977/982 |
| Okuda, et al. | Proceeding of the JapanConcrete Institute | 1996 | 971/976 |
| Komori, et al. | Summaries of technical papers of Annual Meeting, AIJ | 1996 | 679/682 |
| Tada, et al. | Summaries of technical papers of Annual Meeting, AIJ | 1996 | 671/672 |
| Hayashi, et al. | Summaries of technical papers of Annual Meeting, AIJ | 1997 | 385/386 |
| Nagai, et al. | Summaries of technical papers of Annual Meeting, AIJ | 1997 | 371/374 |
| Nkanishi, et al. | Proceeding of the JapanConcrete Institute | 1998 | 679/682 |
| Imaeda, et al. | Summaries of technical papers of Annual Meeting, AIJ | 1998 | 541/544 |
| Shiohara, et al. | Summaries of technical papers of Annual Meeting, AIJ | 1998 | 551/552 |
| Imai, et al. | Summaries of technical papers of Annual Meeting, AIJ | 1999 | 531/536 |
| Tasai, et al. | Summaries of technical papers of Annual Meeting, AIJ | 2000 | 857/860 |
| Matsushima, et al. | Summaries of technical papers of Annual Meeting, AIJ | 2000 | 861/864 |
| Nakazawa, et al. | Summaries of technical papers of Annual Meeting, AIJ | 2001 | 663/664 |
| Hara, et al. | Summaries of technical papers of Annual Meeting, AIJ | 2001 | 247/248 |
| Takeuchi, et al. | Summaries of technical papers of Annual Meeting, AIJ | 2001 | 111/114 |
| Nakazawa, et al. | Proceeding of the JapanConcrete Institute | 2002 | 847/852 |
| Torii, et al. | Summaries of technical papers of Annual Meeting, AIJ | 2003 | 513/516 |
| Kikai, et al. | Proceeding of the JapanConcrete Institute | 2003 | 907/912 |
| Kiyohara, et al. | Summaries of technical papers of Annual Meeting, AIJ | 2004 | 27/34 |
| Sanada, et al. | Proceeding of the JapanConcrete Institute | 2004 | 463/468 |
| Ishiwatari, et al. | Summaries of technical papers of Annual Meeting, AIJ | 2004 | 843/846 |
| Miyashita, et al. | Summaries of technical papers of Annual Meeting, AIJ | 2004 | 861/864 |
| Kiyohara, et al. | Summaries of technical papers of Annual Meeting, AIJ | 2005 | 33/42 |
| Hara, et al. | Summaries of technical papers of Annual Meeting, AIJ | 2005 | 241/244 |
| Imanishi, et al. | Summaries of technical papers of Annual Meeting, AIJ | 2006 | 23/24 |
| Adachi, et al. | Summaries of technical papers of Annual Meeting, AIJ | 2007 | 633/634 |
| Masuo, et al. | Summaries of technical papers of Annual Meeting, AIJ | 2007 | 649/650 |
| Kusunoki, et al. | Summaries of technical papers of Annual Meeting, AIJ | 2008 | 147/150 |
| Shiohara, et al. | Summaries of technical papers of Annual Meeting, AIJ | 2010 | 391/400 |
| Nozaki, et al. | Summaries of technical papers of Annual Meeting, AIJ | 2011 | 533/536 |
| Asai, et al. | Summaries of technical papers of Annual Meeting, AIJ | 2011 | 545/546 |
| Kusuhara, et al. | Proceeding of the JapanConcrete Institute | 2011 | 343/348 |
| Nishimura, et al. | Summaries of technical papers of Annual Meeting, AIJ | 2012 | 481/484 |
| Nishimura, et al. | Summaries of technical papers of Annual Meeting, AIJ | 2013 | 741/744 |
| Masuo, et al. | Summaries of technical papers of Annual Meeting, AIJ | 2013 | 747/748 |
| Nishimura, et al. | Proceeding of the JapanConcrete Institute | 2014 | 187/192 |

Fig. 12 – Axial force ratio vs. joint reinforcement ratio



Fig. 12 shows the relationship between the axial force ratio and the joint reinforcement ratio. The figure is divided into two figures according to the value of column-to-beam bending strength margin. Fig. 12(a) shows the results for a ratio of 1.0 to 1.3, and Fig. 12(b) shows the results for a ratio of 1.3 to 1.8. Moreover, past experimental data are plotted in the figure categorized by the ratio of experimental maximum story shear to calculated value (Exp./Cal.) in addition to experimental results obtained in this paper. Here, Exp./Cal. indicates the ratio of the experimental maximum shear force to the calculated shear force (at the ultimate flexural strength of the beam) from the past research studied listed in Table 4. On the basis of all experimental data, the critical failure zones of the beam-column joint structure are indicated with blue squares and the red sector in the figure. The blue square zones indicate that maximum force of the specimen may not reach story shear force expected by ultimate flexural strength of beam yielding ($\text{Exp./Cal.} < 1.0$) due to a progress of joint yielding. The red sector zone indicates that failure mode of the specimen may lead to axial collapse due to an applying of high-level compressive axial force for the beam-column joint with joint yielding. From the above relationship, it is found that demanded criteria for lateral reinforcement of a joint panel may be predicted with respect to the beam-column joint structures to which a high-level varying axial force is applied. In addition, for a smaller column-to-beam bending ratio, the joint panel failure zone and axial collapse zone become larger, as shown in the figure. However, the number of test specimens to which a high-level axial force was applied was not sufficient to investigate its influence with certainty. The accumulation of data over many experiments and analysis examples will be needed.

5. Conclusion

- a) From the relationship between the story shear force and the shear drift angle of the specimens, the behavior of the beam-column joint structures was significantly different when high-level axial force was applied. It was shown that beam-column joint specimens with a small beam-column strength ratio to which a tensile axial force was applied may not achieve the design expected strength of the specimen. However, this is improved by increasing of the joint reinforcement ratio.
- b) The progress in the shear strain of a joint panel was controlled by subjecting it to a high-level compressive axial force under positive loading. However, the specimen with a small joint reinforcement ratio exhibited significant development of the deformation angle according to the decrease in the shear stress capacity.
- c) The progress in the diagonal maximum crack width in the panel zone was controlled to be relatively small (0.2 to 0.3 mm) until a story deformation drift of 1/50.
- d) From the ultimate failure mode, it was demonstrated that a beam-column joint specimen with a small joint reinforcement ratio, such as the T12-20TC5 specimen, subjected to a high-level varying axial force exhibited significant deterioration in the joint panel zone under negative loading (the application of a tensile axial force) and then axial collapse under positive loading (the application of a compressive axial force).
- e) The influence of the joint reinforcement ratio and varying axial force on the deterioration of the beam-column joint structures as simply illustrated.

6. Acknowledgements

The authors would like to acknowledge the technical support provided by Tokyo Tekko Co., Ltd. and Asahi Industries Co., Ltd. in undertaking the experimental works.

7. References

- [1] Architectural Institute of Japan (1999): Design Guidelines for Earthquake Resistant Reinforced Concrete Buildings Based on Inelastic Displacement Concept.



- [2] Fumio Kusahara and Hitoshi Shiohara (2012): Joint Shear? or Column-to-Beam Strength Ratio? Which is a Key Parameter for Seismic Design of RC Beam-Column Joints - Test Series on Exterior Joints. Proc. 15th World Conference on Earthquake Engineering, Lisbon.
- [3] Fumio Kusahara and Hitoshi Shiohara (2013): Seismic Performance of Reinforced Concrete Exterior Beam-Column Joint with Column-to-Beam Strength Ratio Equal or Near Unity, Journal of Structural and Construction Engineering, AIJ, Vol.78, No.693, pp.1939-1948.
- [4] Yusuke Suzuki, Tetsuro Ohta, Mamoru Ito, Tomohiro Adachi, Joji Sakuta, Masaki Maeda (2013): Effect of Lateral Reinforcement and Axial Force on Structural Performance of Exterior Beam and Column Joints in Reinforced Concrete Buildings, Summaries of Technical Papers of Annual Meeting, Architectural Institute of Japan, pp.361-366.